J. Membrane Biol. 191, 165–178 (2003)
DOI: 10.1007/s00232-002-1052-2

The Journal of
Membrane
Biology

Gating of Cl^- Currents in Protoplasts from the Marine Alga *Valonia utricularis* Depends on the Transmembrane Cl^- Gradient and Is Affected by Enzymatic Cell Wall Degradation

K.-A. Binder*, L.H. Wegner*, M. Heidecker, U. Zimmermann
Lehrstuhl für Biotechnologie der Universität, Biozentrum, Am Hubland, D-97074 Würzburg, Germany

Received: 10 June 2002/Revised: 25 September 2002

Abstract. The electrical properties of protoplasts of the turgor pressure-regulating giant marine alga *Valonia utricularis* were investigated by using the patch-clamp technique. In the whole-cell configuration, large inward currents were elicited by negative-going voltage pulses. The time-dependent component was predominantly carried by Cl^-, as revealed by 'tail current' analysis. When experiments were performed on protoplasts directly after mechanical release from the 'mother cell', small outward currents were additionally observed at membrane voltages more positive than E_{Cl^-}. These outward currents disappeared to a large extent after treatment of the protoplasts with a mixture of cell wall-degrading enzymes. Plots of the chord conductance versus the clamped membrane voltage revealed that enzymatic treatment affected the gating properties. By fitting Boltzmann distributions to the data, a midpoint potential of $+5 \pm 5$ mV ($n = 7$) was obtained in symmetrical Cl^- solutions for mechanically released protoplasts. In contrast, protoplasts treated additionally with enzymes exhibited a midpoint potential of -13 ± 5 mV ($n = 8$). By varying the external and internal Cl^- concentration, gating was also shown to depend on the Cl^- gradient across the plasmalemma both in enzymatically treated and untreated protoplasts. Plotting of the midpoint potential against the Nernst potential of Cl^- rendered a slope less than 1 (0.70 and 0.64, respectively) indicating that gating did not strictly depend on the electrochemical Cl^- gradient. The voltage- and Cl^-- dependence as well as inhibition experiments with 4,4′-diisothiocyanatostilbene-2,2′-disulfonic acid (DIDS) suggested that the Cl^- conductance of the membrane is dominated by the Valonia Anion Channel 1 (VAC1) described by Heidecker, M., Wegner, L.H., Zimmermann, U. 1999: A patch-clamp study of ion channels in protoplasts prepared from the marine alga *Valonia utricularis*. *J. Membrane Biol.* 172:235–247. The relevance of the findings for membrane potential control and turgor regulation in *V. utricularis* as well as the general implications of the data for electrophysiological work on protoplasts (that are usually obtained by enzymatic digestion of plant tissue) are discussed.

Key words: *Valonia* — Protoplast — Patch clamp — Voltage-dependent Cl^- current — Cell wall degradation — Gating

Introduction

Giant marine and pond water algae are classical model systems for the study of ion transport processes that are related to turgor and osmotic pressure regulation phenomena (Zimmermann & Steudle, 1974; Zimmermann, Steudle & Lelkes, 1976; Zimmermann, 1978; Bisson & Kirst, 1995). Because of their size, microelectrode techniques can be applied without irreversible damage of the cells (Okazaki, Shimmen & Tazawa, 1984; Okazaki & Iwasaki, 1992; Beilby & Shepherd, 1996; Shepherd & Beilby, 1999; Stento et al., 2000; for a recent review, *see* Findlay, 2001). Due to the large vacuole occupying more than 95% of the cell volume, microelectrodes are positioned in the vacuole. Thus, the data reflect the electrical response of both the tonoplast and the plasmalemma, which are arranged in series. Wang et al. (1997a) and Ryser et al. (1999) were recently able to separate the individual electrical properties of both membranes in the marine giant algae *Valonia utricularis* and *Ventricaria ventricosa*. By perfusing the vacuole or the bath with the pore-forming antibiotic nystatin, these authors could selectively short-circuit

*Contributed equally to this communication

Correspondence to: U. Zimmermann; email: zimmerma@biozentrum.uni-wuerzburg.de

the tonoplast and the plasmalemma, respectively, thus allowing the measurements of the electrophysiological properties of the individual membranes of turgescent cells. These and other studies (Zimmermann & Steudle, 1974; Zimmermann et al., 1976) have shown that Cl^- and K^+ ion transport processes in the plasmalemma play an important role in the regulation of turgor pressure in *V. utricularis* and *V. ventricosa*.

Complementary information about the electrical and ion transport properties of the plasmalemma of turgorless cells can be obtained by patch-clamp studies after local removal of the cell wall by enzymatic digestion (Schroeder, Raschke & Neher, 1987; Bentrup, 1990; Fairley-Grenot & Assmann, 1992; Hedrich, 1995). In the case of *V. utricularis,* protoplasts can easily be obtained by mechanical and enzymatic means (Wang et al., 1997b). There is a bulk of evidence that the outer membrane of these protoplasts originates from the plasmalemma. By performing experiments on cell-attached and outside-out patches, Heidecker, Wegner & Zimmermann (1999) identified three voltage-gated anion channels (VAC1-3) and one K^+ channel (VKC1). From the frequency of appearance it was concluded that the conductance of the membrane of the turgorless protoplasts is mainly dominated by the hyperpolarization-activated anion channel VAC1.

The dominant role of VAC1 in the conductance of the plasmalemma of protoplasts could be confirmed in the present study by whole-cell configuration measurements. Most importantly, it could be shown that this channel is gated by Cl^- concentration gradients. Furthermore, improvements of the formation of protoplasts from 'mother cells' by mechanical means also allowed the establishment of gigaseals without subsequent enzymatic treatment. Comparison of the data obtained on enzymatically treated and non-treated cells showed that enzymatic treatment significantly changes the voltage dependence of VAC1 gating. This finding is not only of relevance for the extrapolation of the data to turgescent cells of *V. utricularis,* but may also have far-reaching implications for the interpretation of patch-clamp data derived from protoplasts that were prepared by enzymatic digestion of higher plant tissue.

Materials and Methods

Plant Material

Cells of *Valonia utricularis* (collected from the rocky coast of Ischia, Gulf of Naples, Italy) were cultivated in 40-l plexiglas containers in Mediterranean Sea Water (MSW, 1120 mosmol kg^{-1}, pH 8.1) under a 12-hr light/dark period (2 × 36-W Fluora lamps, Osram, Munich, Germany) at 16°C (289°K). The culture medium was continuously aerated and cycled through an activated carbon filter.

Preparation of Protoplasts

For protoplast preparation, cylindrical or elliptical cells with a length of 10–30 mm and a diameter of 3–5 mm were taken. They were dried gently with filter paper and plasmolyzed by exposure to air for about 5 min. Subsequently, the cells were cut by a pair of scissors and the protoplasmic content was squeezed out into the same patch-clamp medium that was used later for studies in the whole-cell configuration. Drying, cutting and squeezing must be performed in a very controlled manner, in particular for the formation of protoplasts that show giga-seals without further enzymatic treatment.

The irregularly shaped, green-coloured protoplasmic aggregates were incubated for 20 min and were then washed two times with bath medium to remove cell wall fragments and other cellular components from the medium. After about 1 hr most of the protoplasts became spherical. Usually, hundreds of protoplasts with diameters ranging from 30–300 μm could be produced from a single 'mother cell'. The protoplasts regenerated to walled cells after about 24 hr and grew in the following months despite the unphysiological media used for their preparation.

Part of the experiments were performed on these mechanically isolated protoplasts about 0.5 to 2 hr after cutting of the 'mother cell'. In other cases, the protoplasts were additionally incubated in a mixture of cell wall-degrading enzymes as described before (Heidecker et al., 1999). The mixture was composed as follows (in % w/v): 0.5 cellulase, 0.1 pectinase, 0.5 hemicellulase, 0.1 lysozyme and 1.5 bovine serum albumin. The osmotic pressure was adjusted with 1:3 diluted MSW; the pH was set to 5.5 with MES (2-[N-morpholino] ethanesulfonic acid). In some experiments pectinase-free enzyme mixtures as well as a protease inhibitor cocktail (10 or 20 μl Protease Inhibitor Cocktail Set III, Calbiochem-Novabiochem, San Diego, CA, in 1 ml enzyme solution) were used.

If not otherwise stated, all chemicals and enzymes were purchased from Sigma (Sigma, St. Louis, MO).

Electrophysiology

Standard patch-clamp experiments were performed in the whole-cell configuration (Hamill et al., 1981). The setup used for these experiments has been described in detail by Heidecker et al. (1999). Patch-clamp pipettes were fabricated from borosilicate glass capillaries (Hilgenberg, Malsfeld). The external diameter of the capillaries was 1.5 mm and the wall thickness 0.25 mm. They were pulled on a two-stage vertical puller (L/M-3P-A, List-Medical, Darmstadt, Germany). Pipette resistances were in the range of 5–20 MΩ in the media used here. Liquid junction potentials were determined as described previously (Barry & Lynch, 1991; Neher, 1992), and were corrected for if the value exceeded ±3 mV. All experiments were performed at room temperature (25°C).

All solutions were filtered through a 0.22-μm filter before use. The composition of the media is shown in Table 1. The pH of pipette and bath media was adjusted by using HEPES/BTP [N-(2-hydroxyethyl)piperazine-N′-(2-ethanesulfonic acid)/1,3-bis[tris-(hydroxy-methyl)-methylamino]propane].

The bath solution B1 and the pipette solution P1 were used in order to establish nearly symmetrical Cl^- conditions. Unfortunately, the absolute concentrations of Cl^-, K^+, and Na^+ in the cytosol of the intact cell and the bath could not be imitated by using ASW as bath and pipette media, because no giga-seals were obtained under these conditions. However, by using B1/P2 the in vivo concentration gradients between cytosol and bath as well as the Nernst potentials of the ions could be approximated.

The anion channel blocker DIDS (4,4′-diisothiocyanatostilbene-2,2′-disulfonic acid; Fluka, Neu-Ulm, Germany) was dissolved in B1 medium at a final concentration of 200 μM.

Table 1. Composition of the media used in this study (concentrations in mM)

	P1	P2	P3	P4	B1	B2	B3
K^+	115	110	115	110	10	10	10
Na^+	10	10		10	100		100
Cl^-	145	30	135	70	150	50	50
Ca^{2+}	0.1	0.1	0.1	0.1	10	10	10
EGTA[1]	1	1	1	1			
Free Ca^{2+}	55×10^{-6}	55×10^{-6}	55×10^{-6}	55×10^{-6}			
Mg^{2+}	10	10	10	10	10	10	10
HEPES	20	20	20	20	10	10	10
$Gluconate^-$		110		70			100
pH	7.0	7.0	7.0	7.0	8.1	8.1	8.1
Osmolality[2]	301	291	281	291	290	280	290
Mannitol						190	

[1] Ethyleneglycol-bis(β-aminoethyl ether) N,N,N′,N′-tetraacetic acid
[2] in mosmol kg^{-1}

For patch-clamp experiments, spherical protoplasts with a diameter of 40–100 μm were selected. When seal resistances larger than 0.7–1.0 GΩ were established, the patch membrane was broken by a suction pulse to obtain the whole-cell configuration. The passive electrical properties of the protoplast membrane were measured in the current-clamp mode. After elimination of capacitive currents, current-voltage relations of the protoplast were measured in the voltage-clamp mode. The actual voltage drop across the membrane (V_M) at a given clamped pipette voltage (V_P) was calculated by subtracting the voltage difference between pipette and cell interior, which depended on the series resistance (R_S). Voltages were corrected according to $V_M = V_P - I_M R_S$. I_M is the whole-cell current flowing across the membrane. Voltages generated in current-clamp experiments were likewise corrected for series resistance errors. For generating current or voltage pulse protocols, the program CLAMPEX (Axon Instruments, Foster City, CA) was used.

Data Analysis

Patch-clamp data were analyzed using the graphic program ORIGIN (Microcal Software, Northampton, MA). When a negative-going voltage step was applied, an instantaneous current component, I_{inst}, was always observed, which was followed by a second, exponentially increasing component. Thus, the overall current response $I(t)$ could be described by the following equation:

$$I(t) = I_{inst} + I_1(1 - \exp(-t/\tau_1)) \quad (1)$$

where τ_1 is the time constant and I_1 the steady-state amplitude of the exponentially increasing current component. For fitting of Eq. 1 to the experimental data, the Levenberg-Marquard algorithm was used. Thereby the first 20–50 data points were omitted to avoid interference with residual capacitive currents. It has to be noted that in some cases the data could be more adequately fitted when two exponential functions with steady-state amplitudes I_1 and I_2 and time constants τ_1 and τ_2 were assumed. In this case, Eq. 2 was used:

$$I(t) = I_{inst} + I_1(1 - \exp(-t/\tau_1)) + I_2(1 - \exp(-t/\tau_2)) \quad (2)$$

Results

Protoplasts of *V. utricularis* are densely packed with chloroplasts and additionally contain a dense layer of vesicles located at the inner surface of the membrane as revealed by staining with the lipophilic probe DPH (diphenyl-1,3,5-hexatriene; Wang et al., 1997b). This layer could affect the charging process of the membrane, in which case a considerable underestimation of the specific membrane capacity would also be expected. In order to exclude such artefacts we determined the area-specific capacity of the outer membrane in the current-clamp mode. The membrane was charged by injection of a 40-pA current pulse of 0.26 sec duration into the protoplast while in the whole-cell configuration. From the relaxation time of the membrane voltage and the surface area (estimated from the diameter of the spherically shaped protoplasts) a specific resistance of $1.09 \pm 0.52\ \Omega\ m^2$ ($n = 20$) and a specific capacity of $0.85 \pm 0.21\ \mu F\ cm^{-2}$ ($n = 20$) were calculated. A similar value for the specific capacity of the plasmalemma of the 'mother cells' was determined by charge pulse-relaxation experiments ($0.77 \pm 0.16\ \mu F\ cm^{-2}$; $n = 10$; Wang et al., 1997a). The agreement of the values was taken as evidence that the dense lipid vesicle layer did not interfere with clamp experiments in the whole-cell configuration.

Current-Voltage Characteristics of Enzymatically Post-treated Protoplasts

Figure 1*A* shows a typical whole-cell configuration experiment performed on an enzymatically post-treated protoplast. Measurements were performed in symmetrical 150 mM Cl^- solutions (B1/P1) immediately after the establishment of the whole-cell configuration. The pipette was precharged to +60 mV by a 1-sec pulse and then clamped successively at increasingly negative voltages for 2 sec. Between two voltage clamps the voltage was adjusted to 0 mV for 1.1 sec before the pipette voltage was returned to +60 mV (*see* inset of Fig. 1*A*). In this way, seal problems were avoided, which regularly occurred when the voltage was kept at +60 mV throughout the experi-

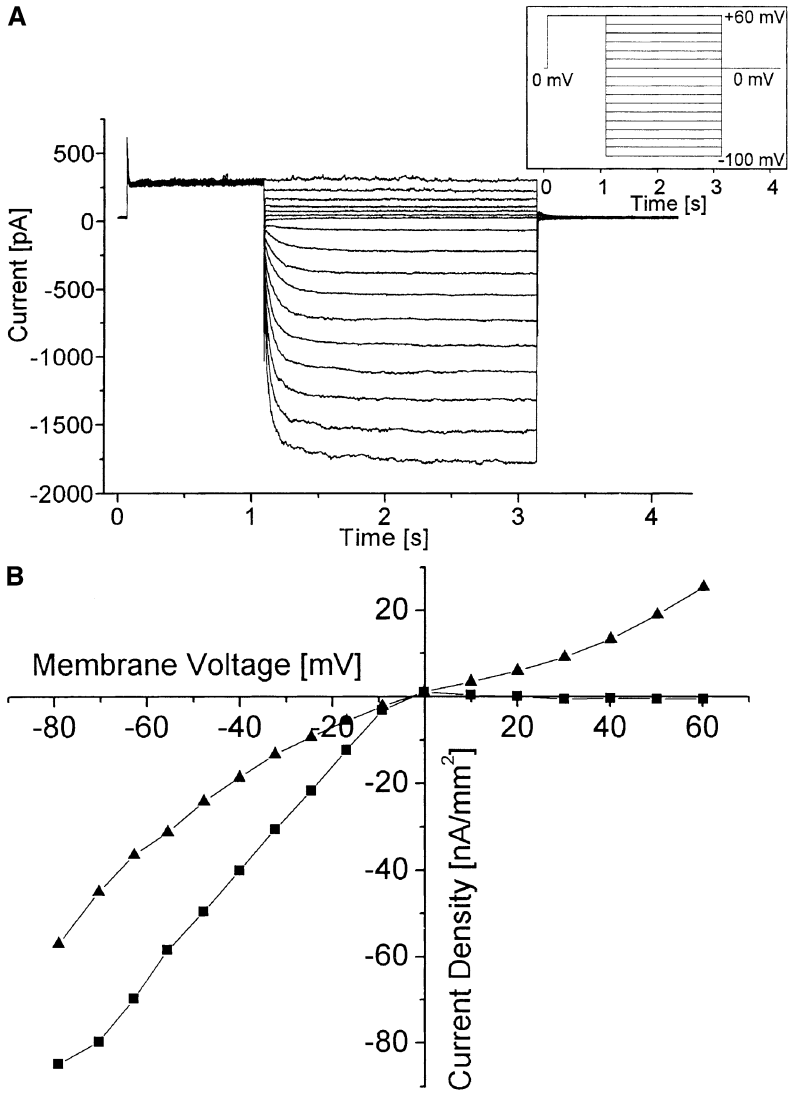

Fig. 1. Typical current-voltage characteristics of an enzymatically treated protoplast of *Valonia utricularis* measured in the whole-cell configuration. Measurements were performed in 150 mM symmetrical Cl^- media (B1/P1). (*A*) Directly after establishment of the whole-cell configuration, the pipette was charged to +60 mV by a current pulse of 1 sec duration and then clamped to a range of more negative voltages. As shown in the inset, pipette voltages were changed in increments of 10 mV and clamped for 2 sec. Between two successive clamps the pipette voltage was adjusted to 0 mV for 1.1 sec before the voltage was returned to +60 mV. As indicated, large, voltage-dependent inward currents were induced when the membrane voltage was clamped at values below zero. The currents were composed of an instantaneously occurring component (▲ in *B*) and of a component (■ in *B*) exponentially increasing with time. (*B*) presents a plot of the two current components (normalized to the surface area) versus the clamped membrane voltage (corrected for the voltage drop across the series resistance). Data were taken from (*A*). Note that the activation potential of the exponential component (showing strong inward rectification properties) was subject to large variations as indicated by corresponding measurements on other protoplasts (*data not shown*). For detailed discussion, *see* text.

ment. As indicated in Fig. 1*A*, large inward currents were induced when the membrane voltage was clamped at negative values. The currents consisted of an instantaneous and of an exponentially increasing component. The time constant τ_1 of the second component was voltage-dependent. From the exponential fits of the data in Fig. 1*A* (by using Eq. 1) τ_1-values were obtained ranging from 0.21 sec (at −9 mV) to 0.06 sec (at −79 mV). The current-voltage relations for both components (normalized to the surface area) are plotted in Fig. 1*B*.

It is obvious that the current-voltage curve of the instantaneous component intersected the voltage axis close to 0 mV. This can be taken as evidence that the seal was not completely perfect and, in turn, that very small leaks around the pipette contributed to this current component (*see* also below). In contrast, the current-voltage characteristics of the exponential component showed strong inward rectification properties. The activation threshold was around 0 mV. Repeated measurements yielded identical results (*data not shown*). Accordingly, similar experiments with other protoplast preparations yielded a similar database (*not shown*), except that sometimes positive currents of very small amplitude could be recorded. These measurements also showed that the activation threshold was subject to large variations. Values down to −20 mV could be measured immediately after the establishment of the whole-cell configuration. However, it is interesting that the threshold usually shifted to more positive values (up to 0 mV) once the measurement was repeated several minutes later. After 15 min no further shift was observed (*data not shown*). An explanation for this unusual shift of the activation threshold was yielded by measurements of the reversal potential, V_{rev}, of the inward rectifier.

To determine the reversal potential, the pulse protocol shown in the inset of Fig. 2*A* was applied to a protoplast clamped in the whole-cell configuration for 20 min. Starting from a holding potential of +30 mV, inward currents were activated by adjusting the pipette voltage to −70 mV. After 1.5 sec the pipette

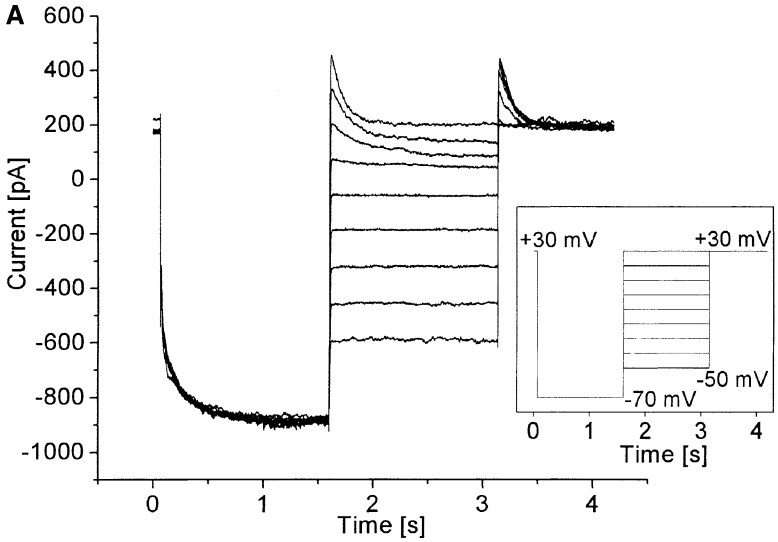

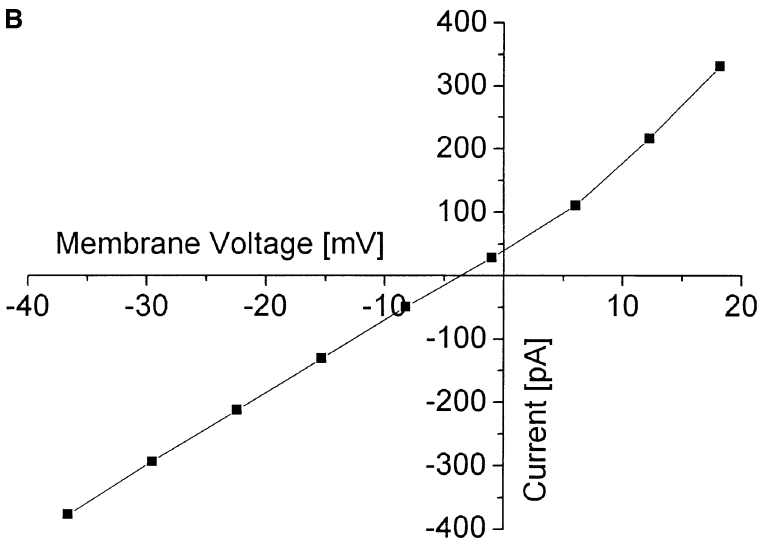

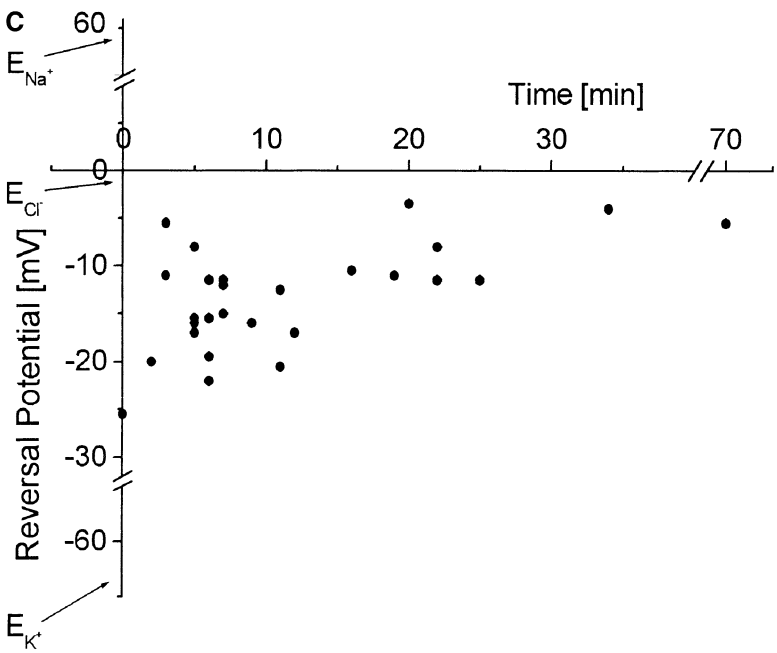

Fig. 2. Typical experiment for the determination of the reversal potential, V_{rev}, of the exponential current component by generation of outward currents. Experimental conditions were identical to those described in Fig. 1*A*, except that the pulse protocol shown in the inset was used. (*A*) Starting from a holding potential of +30 mV, inward currents were induced by clamping the pipette voltage to −70 mV for 1.5 sec. Then the pipette voltage was depolarized in steps of 10 mV to +30 mV. Exponentially decreasing outward currents were generated once positive membrane voltages were established. (*B*) represents the plot of the inward and outward currents versus the corresponding clamped membrane voltage (corrected for series resistance error) by using the data of (*A*). As indicated, the current of this protoplast reversed at −4 mV. (*C*) Cumulative plot of reversal potentials of various protoplasts determined as described in (*A*) as a function of the time elapsed between the establishment of the whole-cell configuration and the beginning of the measurement. Comparison of the 'short-' (< 15 min) and 'long-term' (> 15 min) data suggests that the variations in the reversal potential can be traced back to a (protoplast-dependent) retarded equilibration of the cytosol with the pipette solution (*see* also text). Thus, only for 'short-term' data that agree with 'long-term' data can complete equilibration be assumed. In light of this criterion the reversal potentials are close to the Nernst potential of Cl^- ($E_{Cl^-} = -1$ mV), indicating that the ensemble currents arise from Cl^- channels (see text).

voltage was depolarized successively up to a voltage of +30 mV, as indicated in the inset. Once positive membrane voltages were established, exponentially decaying outward currents were generated through the inward rectifier. The time constant of these 'tail currents' was voltage-dependent and ranged from 0.11 sec (at +18 mV) to 0.50 sec (at −1 mV). The steady-state currents (occurring after the relaxation process was completed) obviously resulted from tiny leaks, as discussed above.

From the exponential fit of the 'tail currents' the initial amplitudes were extrapolated. Plotting of these amplitudes and the amplitudes of the inward currents (corrected for the extrapolated 'leak component') versus the corresponding clamped membrane voltage yielded a nearly linear current-voltage curve (Fig. 2*B*). From the curve, a reversal potential of −4 mV was determined. A cumulative plot of reversal potentials measured on various protoplast preparations and at different periods of time after the establishment of the whole-cell configuration is given in Fig. 2*C*. It is obvious that the values of the reversal potential were subjected to quite a large scatter (ranging from −5 to −25 mV; $n = 25$) when the measurements were performed within 15 min after formation of the whole-cell configuration. This was apparently not the case for whole-cell configurations that were stable for more than 15 min (−4 to −12 mV; $n = 8$).

Considering the shift of the activation threshold (*see* above) and of the reversal potential towards more positive values when time progressed, it seems to be clear that both phenomena are caused by very slow equilibration of the cytosol with the pipette solution in some protoplasts, i.e., that the concentration gradients across the membrane were not well defined at the beginning of the whole-cell clamp. The equilibration problem apparently arose from the exceptionally dense layer of lipid vesicles at the inner surface of the membrane (*see* above), which can vary from protoplast to protoplast (Wang et al., 1997b). Therefore, data of protoplasts in which the 'short-term' measurements differed from the 'long-term' ones, i.e., in which equilibration was obviously retarded, were discarded. In light of this criterion it is clear that the reversal potentials plotted in Fig. 2*C* are close to the Nernst potential of Cl^- ($E_{Cl^-} = -1$ mV), suggesting that the currents measured in the whole-cell configuration apparently represent ensemble currents arising from the hyperpolarization-activated anion channel VAC1 (Heidecker et al., 1999).

Current-Voltage Characteristics of Non-enzymatically versus Enzymatically Treated Protoplasts

Due to the improvement of protoplast preparation (*see* Materials and Methods) a gigaseal could be obtained in about 15% of protoplasts that were not post-treated with enzymes after mechanical preparation. Even though this rate was significantly lower than the number of gigaseals obtained with enzymatically treated protoplasts, the yield was sufficient to study the effect of cell wall-degrading enzymes on the ensemble currents arising from VAC1. Non-treated protoplasts showed a time-dependent shift of the activation threshold and of the reversal potential towards more positive values once the whole-cell configuration had been established, similar to enzymatically treated protoplasts (*data not shown*). Therefore, only those data were included in the analysis that met the criteria outlined above. Averaged current-voltage curves (normalized to the surface area) for untreated ($n = 7$) and treated ($n = 8$) protoplasts are given in Fig. 3*A*. Measurements were performed on the same batches in order to exclude changes of the protoplast properties because of seasonal variations of the physiological properties of the 'mother cells' (*see* Ryser et al., 1999). Inspection of the data in Fig. 3*A* shows that in the case of untreated protoplasts outward currents occurred. These outward currents were regularly observed and significantly larger than the positive currents recorded occasionally in treated protoplasts (*see* above). The positive currents measured in untreated protoplasts assumed a peak value at about +5 mV and decreased then again to zero at a potential of about +20 mV. One explanation for the different behavior of treated and untreated protoplasts could be that enzymatic treatment blocks outward currents (which would be equivalent to Cl^- influx). However, this is not in accordance with the outward current data measured on treated protoplasts (*see* Figs. 2*A*, *B*). An alternative explanation would be that the voltage dependence of gating is affected by enzymatic treatment. Calculation of the chord conductances, G, which reflect the voltage dependence of channel activity, supported this hypothesis, shown in Fig. 3*B*. The dependence of the chord conductances [defined by $G = I/(V_M - V_{rev})$] on the corresponding clamped membrane voltage, V_M, was obtained by using the data shown in Fig. 3*A*. Comparison of the curves of treated and untreated protoplasts shows that enzymatic treatment shifts the chord conductance-voltage curve to more negative potentials (by about −18 mV). When pectinase-free enzyme mixtures were used, the shift of the curves was less (by about −11 mV; $n = 3$), indicating that this enzyme contributed significantly to the effect. Addition of a protease inhibitor cocktail had only an effect on the shift in one out of six experiments (*data not shown*), thus leaving the question open whether protease activity in the commercially available enzyme preparations was responsible.

Because of the linear relationship between the 'tail currents' and the clamped membrane voltage, the

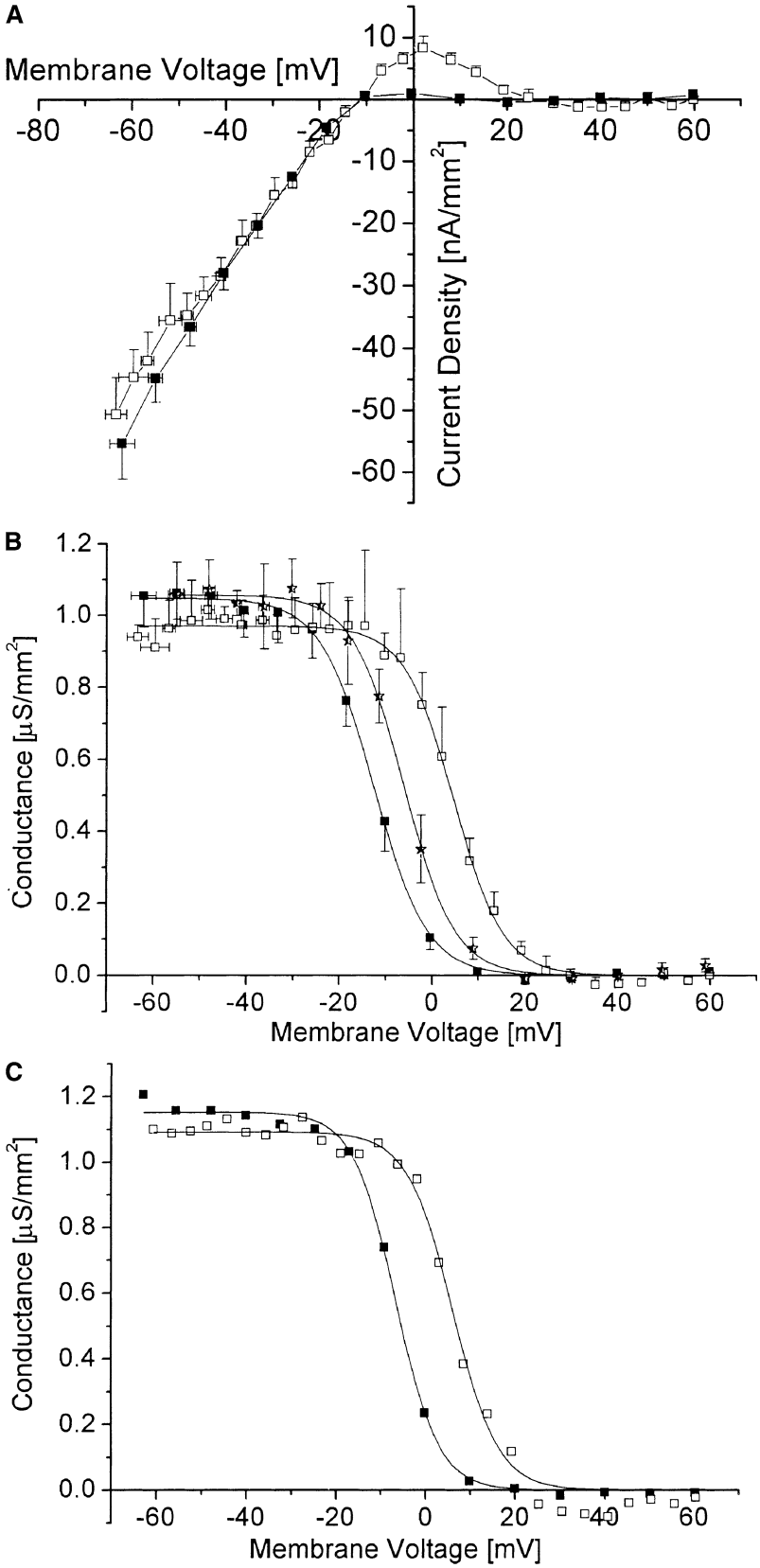

Fig. 3. Comparison of measurements performed on untreated and enzymatically post-treated protoplasts. (*A*) Current-voltage characteristics of enzymatically post-treated versus untreated *V. utricularis* protoplasts by using the experimental whole-cell configuration conditions as described in Fig. 1*A*. Comparison of the data (means ± SE) of untreated (□; $n = 7$) and treated protoplasts (■; $n = 8$) shows that outward currents (with a peak value around +5 mV) occurred when the enzymatic treatment was omitted. (*B*) Plot of the mean chord conductances versus the corresponding clamped membrane voltage calculated from the data shown in (*A*). Additionally, data are given from current-voltage characteristics measured on protoplasts that were treated with a pectinase-free enzyme mixture (★; $n = 3$). The curves represent fits of Boltzmann distributions (according to Eq. 3). The slope factors (S; in mV^{-1}) and the midpoint potentials ($V_{1/2}$; in mV) deduced from the fits were for untreated protoplasts, −0.19/+5, for treated protoplasts, −0.17/−13 and for protoplasts treated with pectinase-free enzyme mixtures, −0.18/−6. (*C*) represents a plot of the chord conductance versus the corresponding clamped membrane voltage measured on an individual protoplast before (□) and after (■) exposure to the enzyme mixture. The Boltzmann fits yielded slope factors of −0.20 mV^{-1} and −0.21 mV^{-1} and midpoint potentials of +6 mV and −7 mV, respectively.

averaged conductance-voltage curves in Fig. 3*B* could be fitted by the Boltzmann function:

$$G = \frac{G_{max}}{1 + \exp -(S(V_M - V_{1/2}))} \quad (3)$$

where V_M is the clamped membrane voltage; S is the slope factor, and $V_{1/2}$ is the membrane voltage at which the conductance was 50% of the maximum value (i.e., the midpoint potential).

As indicated, the three curves exhibited almost identical slope factors; i.e., -0.19 mV^{-1} ($n = 7$) for untreated versus -0.17 mV^{-1} ($n = 8$) and -0.18 mV^{-1} ($n = 3$) for protoplasts treated with the complete and with the pectinase-free enzyme mixture, respectively. This finding can be taken as evidence that the number of mobile charges involved in voltage sensing is not affected by enzyme treatment. Similarly, the maximum conductances did not differ significantly, indicating that the number of active channels and the single channel conductance were not affected. In contrast, the midpoint potentials differed significantly (+5 mV for untreated protoplasts; -13 mV and -6 mV for the treated protoplasts), suggesting that the voltage sensor was affected by exposure of the membrane to cell wall-degrading enzymes.[1]

The above findings and conclusions were supported by measurements in which the current-voltage characteristic of an individual protoplast was determined before and after enzymatic treatment. A typical voltage-dependence of the chord conductance calculated from such data is shown in Fig. 3*C*. In accordance with the data depicted in Figs. 3*A* and *B*, the maximum conductance and the slope factor remained unaffected upon enzymatic treatment, whereas the midpoint potential shifted from +6 mV to -7 mV. On average, the shift of the midpoint potential was -18 ± 5 mV ($n = 4$).

The results demonstrate that artefact-free identification of the channel contributing to the ensemble currents recorded in the whole-cell configuration can only be expected if enzymatic post-treatment is avoided. Thus, if not otherwise stated, the following measurements were performed with untreated protoplasts.

[1]From the fits of the individual conductance-voltage curves the following average values ±SD for the slopes (S in mV^{-1}) and the midpoint potentials ($V_{1/2}$ in mV) were obtained: -0.21 ± 0.07/ $+5 \pm 5$ for untreated protoplasts ($n = 7$); -0.19 ± 0.02/ -13 ± 5 with the complete enzymc mixture ($n = 8$) and -0.21 ± 0.06/ -6 ± 3 for protoplasts treated with pectinase-free enzyme mixture ($n = 3$).

VAC1 Dominates the Membrane Conductance and Is Gated by Cl^- Concentration Gradients

Support for the above conclusion that VAC1 contributed mainly to the current in the whole-cell configuration came from measurements on untreated protoplasts in the presence of Cl^- concentration gradients, as well as after addition of the Cl^- channel inhibitor DIDS. As described in Materials and Methods, Cl^- gradients were established by using 150 mM Cl^- in the bath and 30 mM Cl^- in the pipette (B1/P2). As shown in Fig. 4 for a representative measurement (○), the Cl^- gradient shifts the reversal potential to more negative values in comparison to the symmetrical conditions. On average, the reversal potential was -37 ± 3 mV ($n = 7$) and thus close to the Nernst potential of Cl^- (-41 mV), supporting the above view that the current in the whole-cell configuration is dominated by this anion (*see* also Heidecker et al., 1999). Consistently, after addition of 200 μM DIDS to the bath, the amplitude of inward currents decreased almost linearly (Fig. 4) until after 37 min final values were reached that corresponded to 10–20% of the original values. The inhibition was voltage-independent. Similar results were obtained in four other independent experiments. Control measurements in which the current-voltage characteristics were determined repeatedly over a period of at least 20 min gave no indication that the reduction of current was due to a rundown effect. Artefacts arising from the exchange of the bath medium against the DIDS-containing medium could also be excluded (*data not shown*).

Further support for the hypothesis that current in the whole-cell configuration is mainly carried by Cl^-, arrived from current-voltage characteristics measured at various Cl^- gradients (Fig. 5*A*). When Cl^- in the bath was kept at 150 mM and Cl^- in the pipette was adjusted to 30, 70 and 145 mM, respectively (solutions P2, P4 and P1; *see* Table 1) large inward currents were observed at clamped membrane voltages being more negative than the reversal potential (comparable to Fig. 1*B*). Independent of the imposed Cl^- gradients, outward currents always occurred (up to membrane voltages of about $V_M = V_{rev} + 30$ mV; Fig. 5*A*). These currents exhibited peak values, as already shown in Fig. 3*A*.

The values of the reversal potentials for these combinations of bath and pipette solutions were determined to be -37 ± 3 mV ($n = 7$), -23 ± 6 mV ($n = 4$) and -9 ± 3 mV ($n = 12$), respectively. These values were close to the corresponding Nernst potentials of Cl^- of -41, -19 and -1 mV. Satisfactory agreement between the reversal potential and the Nernst potential of Cl^- was also obtained when Cl^- in the bath and in the pipette solution was adjusted to 50 mM and 135 mM, respectively (B2/P3;

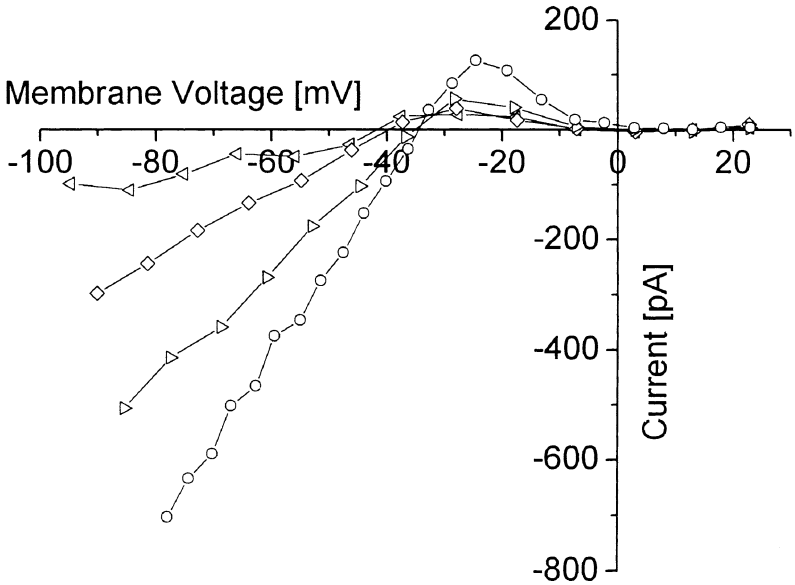

Fig. 4. Effect of DIDS on current-voltage characteristics of an untreated protoplast in the presence of a 150/30 mM Cl^- gradient. Current-voltage curves were recorded before (○) and 15 min (▷), 29 min (◇) and 37 min (◁) after addition of 0.2 mM DIDS to the bath. The same experimental conditions were used as described in Fig. 1 except that the control currents were scanned in 5-mV increments. The voltage values were corrected for the junction potential, which was determined to be −7 mV in this experiment and for the voltage drop across the series resistance. Note that the reversal potential of the control curve (−35 mV) shifted upon addition of DIDS to a value of −41 mV, which corresponds to the Nernst potential of Cl^-.

V_{rev} = +13 ± 3 mV, n = 10; E_{Cl^-} = +25 mV). These results strongly suggest that Cl^- was the main but possibly not the only permeant ion. A few experiments with media in which K^+ or Na^+ were omitted showed that these ions did not contribute significantly to the whole-cell currents. Thus, the reason for the deviation of the reversal potential from the Nernst potential of Cl^- remains unresolved.

Fig. 5*B* shows the chord conductances (normalized to the maximum value) in dependence of the clamped membrane voltage for the various Cl^- gradients. Since the 'tail currents' depended linearly on the clamped membrane voltage around the midpoint potential (*data not shown*) the data could be fitted by Boltzmann distributions. Inspection of the fitted curves indicated that the slope was gradient-independent, but that the midpoint potential was apparently correlated with the Nernst potential of Cl^-. Combinations of pipette and bath solutions were chosen in such a way that dependence of gating on the internal or external Cl^- concentrations alone could be excluded. In Fig. 5*C* the midpoint potentials are plotted as a function of the Nernst potential of Cl^-. Simultaneously, the corresponding midpoint potentials measured on enzymatically treated protoplasts in the same manner as described above (*data not shown*) are presented in dependence on the Nernst potential of Cl^-. Linear relationships were obviously obtained for both protoplast preparations. The slopes of both curves were with 0.64 ± 0.06 (untreated) and 0.70 ± 0.08 (treated) nearly identical. However, exposure of the membrane to cell wall-degrading enzymes apparently resulted in a strong shift towards negative values (by about −18 mV). Taking into account the data obtained under symmetrical Cl^- conditions (*see* Fig. 3), it is clear that the effect of enzymatic treatment on the voltage gating of VAC1 is independent of the imposed Cl^- gradients.

Discussion

By employing the whole-cell patch-clamp technique we have demonstrated here that the membrane conductance of protoplasts isolated from the unicellular marine alga *Valonia utricularis* is dominated by a Cl^- selective inward rectifier. This is supported by the magnitude of the reversal potential (Fig. 2) and by the Cl^- -gradient dependence (Fig. 5). This finding is in agreement with a previous study on Cl^- channel activity in cell-attached and outside-out patches of enzymatically treated protoplasts of *V. utricularis* (Heidecker et al., 1999). Furthermore, the whole-cell data strongly suggest that inward Cl^- currents result predominantly, if not entirely, from the activity of the Cl^- channel VAC1 previously characterized in cell-attached and outside-out patches of *V. utricularis* protoplasts (Heidecker et al., 1999). As in the case of VAC1, whole-cell Cl^- currents were inhibited by the anion channel blocker DIDS and were activated by a hyperpolarization of the protoplast membrane. In addition, the Boltzmann analysis gave clear-cut evidence that this resulted from a strong voltage-dependence of gating. Estimation of the macroscopic current-voltage curves by using VAC1 parameters (extracted from current fluctuations in outside-out patches; Heidecker et al., 1999) show very good agreement with the whole-cell data measured on enzymatically treated protoplasts (for details, *see* legend to Fig. 6). This can be taken as further evidence that whole-cell Cl^- currents resulted from VAC1 activity. This allows a rough estimation of the channel density in enzy-

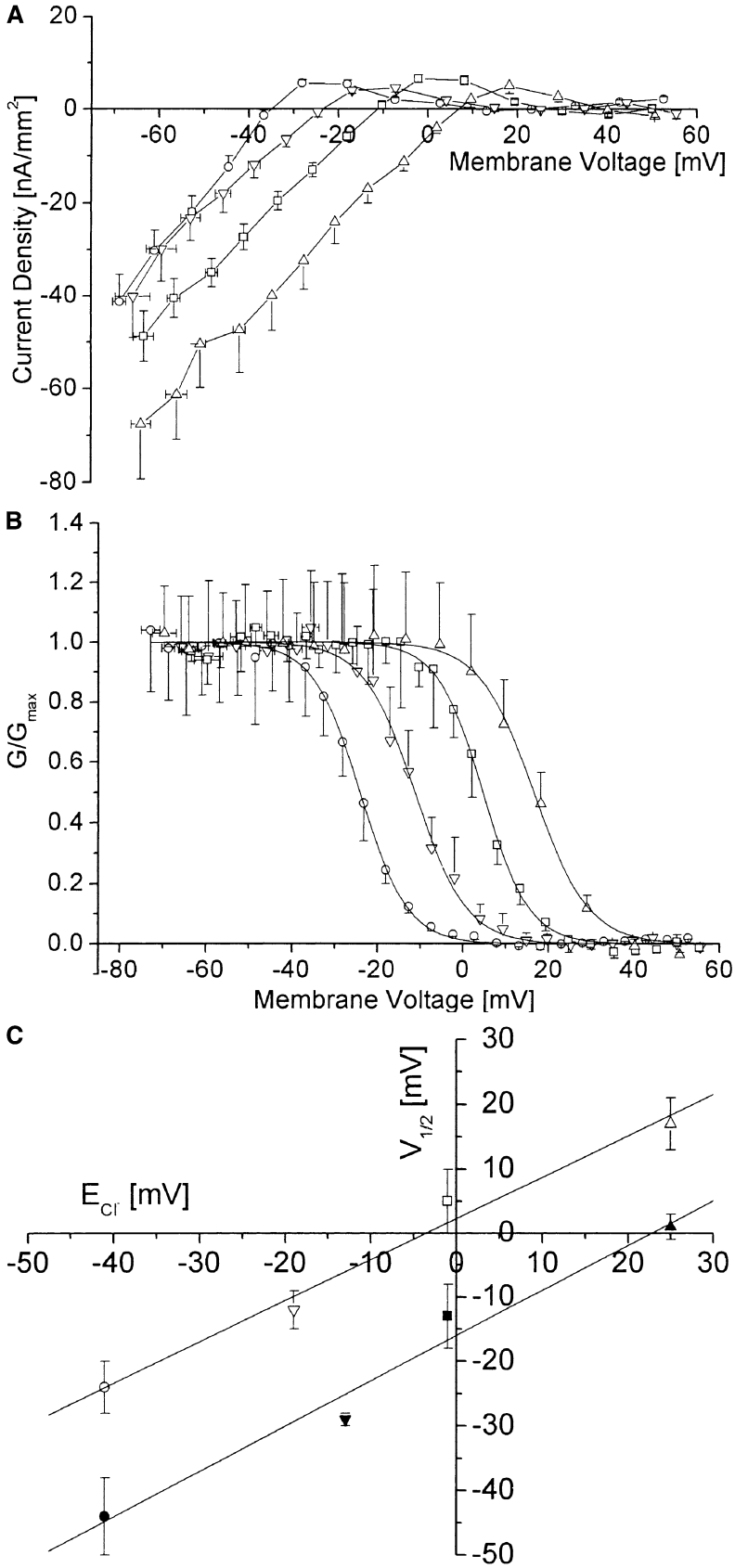

Fig. 5. Influence of Cl^- gradients on the midpoint potential. (*A*) Effect of Cl^- gradients on the current-voltage characteristics of untreated protoplasts. Pulse conditions were identical to those described in Fig. 1*A*. Gradients were established by using the media listed in Table 1. Data represent means ± SE. Voltages were corrected for junction potentials and series resistance errors. Symbols: Δ (B2/P3; $E_{Cl^-} = +25$ mV; $n = 5$), □ (B1/P1; $E_{Cl^-} = -1$ mV; n = 7), ∇ (B1/P4; $E_{Cl^-} = -19$ mV; $n = 3$) and ○ (B1/P2 media; $E_{Cl^-} = -41$ mV; $n = 8$). Note the gradient-independent occurrence of outward currents. (*B*) represents G/G_{max}, i.e., the chord conductances normalized to the maximum conductance at each gradient, in dependence on the corresponding membrane voltage. From the fits of Boltzmann distributions to the averaged data, slope factors (in mV^{-1}) of −0.16 (Δ),−0.19 (□),−0.17 (∇) and −0.18 (○) were derived. The corresponding midpoint potentials, $V_{1/2}$ (in mV, mean values ± SD) are given in (*C*) as a function of the Nernst potential of Cl^-. Additionally, the corresponding data for enzymatically post-treated protoplasts are presented (filled symbols). These data were extracted from measurements performed as described in (*A*). Symbols: ▲ (B2/P3; $E_{Cl^-} = +25$ mV; $n = 3$), ■ (B1/P1; $E_{Cl^-} = -1$ mV; $n = 8$), ▼ (B3/P2; $E_{Cl^-} = -13$ mV; $n = 3$) and ● (B1/P2; $E_{Cl^-} = -41$ mV; $n = 5$). The data points were fitted by linear regression. The slope of the curves was 0.64 and 0.70 and the ordinate was intersected at +2.3 mV and −16.0 mV respectively, indicating that enzymatic treatment shifts the function $V_{1/2} = f(E_{Cl^-})$ to more negative values.

matically treated protoplasts. By dividing the averaged maximum whole-cell conductances by the mean single-channel conductances in the outside-out configuration, channel densities of 29100 mm^{-2} for symmetrical (B1/P1 media) and 50900 mm^{-2} for asymmetrical Cl^- conditions (B1/P2 media) are obtained. Even though the order of magnitude is similar, the difference in the values is somewhat large. The reason for this is not known, but may be related to unknown regulation processes of Cl^- transport.

Despite the good agreement with the whole-cell and outside-out data, there are small inconsistencies with the data deduced from cell-attached patches made from enzymatically treated protoplasts (Heidecker et al., 1999). Whereas VAC1 carried outward currents at membrane voltages more positive than the Nernst potential of Cl^-, significant outward currents were not observed in the whole-cell configuration. Such currents occurred only when enzymatic treatment was omitted. This may be due to the loss of cytoplasmic factors during preparation of the outside-out and whole-cell configuration from enzymatically treated protoplasts. The explanation is supported by previous findings of Heidecker et al. (1999) that Cl^- channel activity in the intact protoplast was enhanced in comparison to outside-out patches. Enzymatic effects can be excluded as a possible explanation for the controversial results because they stand in contrast to the finding that outward currents occurred in the whole-cell configuration of untreated cells (*see* Fig. 3*A*). However, the Boltzmann analysis of the conductance-voltage curves of untreated protoplasts gave evidence that the enzyme mixture modified the midpoint potential and, therefore, the voltage sensor resulting in an activation of the Cl^- currents at more negative potentials. Since other electrical properties remained unaffected, this finding shows that the effect of the enzymes on the channel protein was highly specific. Therefore, it is quite conceivable that these interactions of the enzymes with VAC1 may lead occasionally to the formation of VAC3 recently described by Heidecker et al. (1999) for attached and outside-out configurations. The frequency of appearance of this channel was quite low, but VAC3 exhibited the same conductance as VAC1. Pectinase (or rather the commercially available, enriched pectinase preparation) was apparently one of the main enzymes that interacted specifically with VAC1, because the shift of the midpoint potential was less dramatic when pectinase was omitted in the enzyme mixture. Even though the voltage dependence of the chord conductance was not affected by addition of a protease-inhibitor cocktail to the enzyme mixture in a reproducable way, protease contaminations within the enzyme mixture cannot definitely be excluded as further candidates for the observed shift of the chord conductance upon voltage.

To our knowledge there is no literature dealing with the effect of cell wall-degrading enzymes on channel properties of plant protoplasts. However, some indirect information is available. For example, whole-cell measurements on intact guard cells (Blatt, 1991; Grabov & Blatt, 1998) and on guard cell protoplasts (Schroeder et al., 1987; Fairley-Grenot & Assmann, 1992; Hedrich, 1995) gave results that agreed remarkably well. On the other hand, patch-clamping of intact guard cells in which the cell wall was locally removed by laser microsurgery (De Boer et al., 1994) contrasted the results obtained on protoplasts (Henriksen et al., 1996). Therefore, whether the findings reported here for protoplasts arising from a marine alga have a general impact for patch-clamp studies on plant protoplasts cannot be decided at the present state of the art.

A further interesting feature of the Cl^- currents carried by VAC1 in *V. utricularis* protoplasts is that they were gated by Cl^- concentration gradients. Such a gradient dependence of Cl^- channels is not reported for algae (Coleman, 1986; Tyerman, Findlay & Paterson, 1986a,b; Beilby & Shepherd, 1996; McCulloch, Laver & Walker, 1997; Shepherd & Beilby, 1999) and for higher plant protoplasts (Elzenga & Van Volkenburgh, 1997; for a review, *see* Barbier-Brygoo et al., 2000). To our knowledge, there is only one report on guard-cell protoplasts that describes an activation of inward Cl^- currents by external Cl^- (Hedrich & Marten, 1993; *see also* the review of Hedrich, 1994); however, this was shown to be due to an increase of the single-channel conductance rather than a modulation of gating. From extensive studies on Cl^- channels of mammalian cells belonging to the ClC family, it is also not known that voltage dependence of gating is controlled by Cl^- gradients, but in most experiments, gating was studied by variation of either the internal or external Cl^- concentration (Pusch et al., 1995, 1999; Jordt & Jentsch, 1997; Friedrich, Breiderhoff & Jentsch, 1999; for a review *see* Jentsch et al., 1999). For example, for the Cl^- channel C1C0 in *Torpedo electropax,* Pusch et al. (1995) showed that the midpoint potential of the 'fast' gate activated by depolarization depended on the external, but not on the internal Cl^- concentration. In contrast, voltage dependence of the hyperpolarization-activated 'slow' gate of C1C0 as well as gating of C1C2, which is almost ubiquitously expressed in mammalian cells (Jordt & Jentsch, 1997), was modulated by internal but not external Cl^- (Pusch et al., 1999). Thus, gating by Cl^- gradients appears to be a unique property of VAC1. Due to the gradient- and voltage-dependence of the gating of VAC1, the Cl^- fluxes are not affected significantly by changes in the concentration gradients, but dramatically by changes in the membrane potential around the Nernst potential. This is in agreement with results

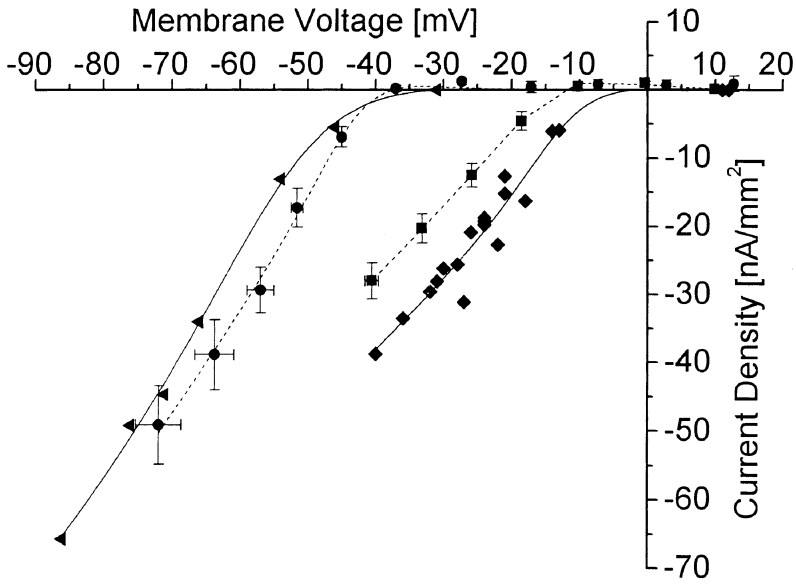

Fig. 6. Current-voltage characteristics (normalized to the surface area) calculated from VAC1 currents measured in the outside-out configuration at symmetrical B1/P1 (◆) and asymmetrical (◀) B1/P2 Cl^- conditions in comparison to the corresponding whole-cell current-voltage characteristics (■ and ●, respectively). Data were taken from Fig. 3*A* in Heidecker et al. (1999) and from the whole-cell measurements on treated protoplasts used in Fig. 5*C* for the calculation of $V_{1/2}$, respectively. The data were fitted by using the equation $I_M(V) = n\, p_o(V)\, g\, (V_M - V_{rev})$, where n = number of channels per surface area, p_o = open probability, and g = single channel conductance. For the ensemble currents in the whole-cell configuration, the open probability as a function of membrane voltage was calculated from $G/G_{max} = f(V_M)$ by using Eq. 3. From the fit of the outside-out data, the midpoint potentials (in mV) and slope factors (in mV^{-1}) were calculated to be −12/−0.23 for symmetrical and −54/−0.12 for asymmetrical Cl^- conditions. The corresponding values for the whole-cell data were −13/−0.22 and −43/−0.25, respectively. The very good agreement of the data supports the view that whole-cell currents are dominated by VAC1. For further discussion, *see* text.

obtained on the 'mother cells' (Heidecker et al., manuscript in preparation).

However, it has to be pointed out that the gating of VAC1 is apparently not under tight control of the electrochemical Cl^- potential gradient because plotting of the midpoint potentials against the Nernst potentials of Cl^- did not yield a slope of one (as expected for tight coupling); rather smaller values of 0.64 (untreated protoplasts) and 0.70 (treated protoplasts) were found (Fig. 5*C*). This means that a tenfold increase in external or internal Cl^- concentration was only equivalent to a change of about ±40 mV (and not of ±59 mV) of the membrane potential. An explanation for this could be that other ions (e.g., K^+) interfere with the gating of VAC1 (*see* below). It is, however, also possible that tight coupling exists, but that the high density of chloroplasts and/or lipid vesicles within the protoplasts (associated with large unstirred layers) results in the formation of internal Cl^- gradients. In this case, it is conceivable that the internal Cl^- concentration at the membrane is smaller than assumed, leading to an underestimation of the slope of the midpoint potential versus the Nernst potential of Cl^-. A plot of the midpoint potentials versus the reversal potential yields (*data not shown*) a slope value closer to 1 (0.93 for treated and 0.84 for untreated protoplasts). This finding is consistent with both explanations.

Independent of the correct explanation, the question is, how can concentration gradients gate the Cl^- channel. A possible mechanism is suggested by the models of Richard & Miller (1990) and Pusch et al. (1995). In light of experimental evidence on CIC channels, these authors assume that the channel gate is under control of a Cl^- binding site within the pore. Therefore, concentration gradients can come into play if two binding sites exist, one accessible for internal and the other one for external Cl^-. This hypothesis shows that one of the next steps in the elucidation of the mechanism of turgor pressure regulation must include cloning of VAC1 and site-directed mutagenesis of the channel as well as studies on the role of Cl^- gradients in turgor pressure regulation of walled protoplasts and the 'mother cells'.

Finally, a surprising result is that the membrane barrier of the 'mother cells' (from which the protoplast membrane originates) was shown to conduct K^+ in dependence on turgor pressure, in particular upon approaching a turgor pressure of zero MPa (Gutknecht, 1968; Zimmermann, Büchner & Benz, 1982). Cl^- fluxes were only weakly pressure-dependent despite the coupling of Cl^- and K^+ fluxes due to the requirement of electroneutrality. Different from other algae (Bentrup, 1990), in *V. utricularis* protoplasts we have not found any evidence for K^+ channel activity in the whole-cell configuration with the media listed in Table 1 nor with solutions lacking Na^+. The reason for this is unknown, but it is conceivable that the pressure dependence of the K^+ fluxes may arise from the electromechanical and kinetic interplay of the tonoplast with the plasmalemma (*see* Coster, Steudle & Zimmermann, 1978).

This work was supported by a grant from the Deutsche Forschungsgemeinschaft (Zi 99/13-1) to U. Z.

References

Barbier-Brygoo, H., Vingauer, M., Colcombet, J., Ephritikine, G., Frachisse, J.-M, Maurel, C. 2000. Anion channels in higher plants: Functional characterization, molecular structure and physiological role. *Biochim. Biophys. Acta* **1465:**199–218

Barry, P.H., Lynch, J.W. 1991. Liquid junction potentials and small cell effects in patch-clamp analysis. *J. Membrane Biol.* **121:**101–117

Beilby, M.J., Shepherd, V.A. 1996. Turgor regulation in *Lamprothamnium papulosum*. I. I/V analysis and pharmacological dissection of the hypotonic effect. *Plant Cell Environ.* **19:**837–847

Bentrup, F.W. 1990. Potassium ion channels in the plasmalemma. *Physiol. Plant.* **79:**705–711

Bisson, M.A., Kirst, G.O. 1995. Osmotic acclimation and turgor pressure regulation in algae. *Naturwissenschaften* **82:**461–471

Blatt, M.R. 1991. Ion channel gating in plants: Physiological implications and integration for stomatal function. *J. Membrane Biol.* **124:**95–112

Coleman, H.A. 1986. Chloride currents in *Chara* — a patch-clamp study. *J. Membrane Biol.* **93:**55–63

Coster, H.G.L., Steudle, E., Zimmermann, U. 1978. Turgor pressure sensing in plant cell membranes. *Plant Physiol.* **58:**636–643

De Boer, A.H., van Duijn, B., Giesberg, P., Wegner, L.H., Obermeyer, G., Köhler, K., Linz, K.W. 1994. Laser microsurgery: a versatile tool in plant (electro)physiology. *Protoplasma* **178:**1–10

Elzenga, J.T.M., Van Volkenburgh, E. 1997. Kinetics of Ca^{2+} -and ATP-dependent, voltage-controlled anion conductance in the plasma membrane of mesophyll cells of *Pisum sativum*. *Planta* **201:**415–423

Fairley-Grenot, K., Assmann, S.M. 1992. Whole cell K^+ current across the plasma membrane of guard cells from a grass: *Zea mays*. *Planta* **186:**282–293

Findlay, G.P. 2001. Membranes and electrophysiology of turgor regulation. *Aust. J. Plant Physiol.* **28:**617–634

Friedrich, T., Breiderhoff, T., Jentsch, T.J. 1999. Mutational analysis demonstrates that CIC-4 and CIC-5 directly mediate plasma membrane currents. *J. Biol. Chem.* **274:**896–902

Grabov, A., Blatt, M.R. 1998. Co-ordination of signalling elements in guard cell ion channel control. *J. Exp. Bot.* **49:**351–360

Gutknecht, J. 1968. Salt transport in *Valonia:* Inhibition of potassium uptake by small hydrostatic pressures. *Science* **160:**68–70

Hamill, O.P., Marty, A., Neher, E., Sakmann, B., Sigworth, F.J. 1981. Improved patch-clamp techniques for high-resolution current recording from cells and cell-free membrane patches. *Pfluegers Arch.* **391:**85–100

Hechenberger, M., Schwappach, B., Fischer, W.N., Frommer, W.B., Jentsch, T.J., Steinmeyer, K. 1996. A family of putative chloride channels from *Arabidopsis* and functional complementation of a yeast strain with a CLC Gene disruption. *J. Biol. Chem.* **271:**33632–33638

Hedrich, R. 1994. Voltage-dependent chloride channels in plant cells: Identification, characterization, and regulation of a guard cell anion channel. *Curr. Top. Membr.* **42:**1–33

Hedrich, R. 1995. Technical approaches to studying specific properties of ion channels in plants. *In*: Single channel recording. B. Sakmann and E. Neher, editors, pp. 277-305. 2nd edition, Plenum Press, New York

Hedrich, R., Marten, I. 1993. Malate-induced feedback regulation of plasma membrane anion channels could provide a CO_2 sensor to guard cells. *EMBO J.* **12:**897–901

Heidecker, M., Wegner, L.H., Zimmermann, U. 1999. A patch-clamp study of ion channels in protoplasts prepared from the marine alga *Valonia utricularis*. *J. Membrane Biol.* **172**:235–247

Henriksen, G.H., Taylor, A.R., Brownlee, C., Assmann, S.M. 1996. Laser microsurgery of higher plant cell walls permits patch-clamp access. *Plant Physiol.* **110:**1063–1068

Jentsch, T.J., Friedrich, T., Schriever, A., Yamada, H. 1999. The CLC chloride channel family. *Pfluegers Arch.— Eur. J. Physiol.* **437:**783–795

Jordt, S.-E., Jentsch, T.J. 1997. Molecular dissection of gating in the C1C-2 chloride channel. *EMBO J.* **16:**1582–1592

McCulloch, S.R., Laver, D.R., Walker, N.A. 1997. Anion channel activity in the *Chara* plasma membrane: co-operative subunit phenomena and a model. *J. Exp. Bot.* **48:**383–397

Neher, E. 1992. Corrections for liquid junction potentials in patch clamp experiments. *Methods Enzymol.* **207:**123–130

Okazaki, Y., Iwasaki, N. 1992. Net efflux of Cl^- during hypotonic turgor regulation in a brackish water alga *Lamprothamnium*. *Plant Cell Environ.* **15:**61–70

Okazaki, Y., Shimmen, T., Tazawa, M. 1984. Turgor regulation in brackish charophyte, *Lamprothamnium succinctum*. II. Changes in K^+, Na^+ and Cl^- concentrations, membrane potential and membrane resistance during turgor regulation. *Plant Cell Physiol.* **25:**573–581

Pusch, M., Jordt, S.-E., Stein, V., Jentsch, T.J. 1999. Chloride dependence of hyperpolarization-activated chloride channel gates. *J. Physiol.* **515:**341–353

Pusch, M., Ludewig, U., Rehfeldt, A., Jentsch, T.J. 1995. Gating of the voltage-dependent chloride channel ClC-0 by the permeant anion. *Nature* **373:**527–531

Richard, E.A., Miller, C. 1990. Steady-state coupling of ion-channel conformations to a transmembrane ion gradient. *Science* **247:**1208–1210

Ryser, C., Wang, J., Mimietz, S., Zimmermann, U. 1999. Determination of the individual electrical and transport properties of the plasmalemma and the tonoplast of the giant marine alga *Ventricaria ventricosa* by means of the integrated perfusion/charge-pulse technique: evidence for a multifolded tonoplast. *J. Membrane Biol.* **168:**183–197

Schroeder, J.I., Raschke, K., Neher, E. 1987. Voltage dependence of K^+ channels in guard-cell protoplasts. *Proc. Natl. Acad. Sci. USA* **84:**4108–4112

Shepherd, V.A., Beilby, M.J. 1999. The effect of an extracellular mucilage on the response to osmotic shock in the charophyte alga *Larnprothamnium papulosum*. *J. Membrane Biol.* **170:**229–242

Stento, N.A., Gerber Ryba, N., Kiegle, E.A., Bisson, M.A. 2000. Turgor regulation in the salt-tolerant alga *Chara longifolia*. *Plant Cell Environ.* **23:**629–637

Tyerman, S.D., Findlay, G.P., Paterson, G.J. 1986a. Inward membrane current in *Chara inflata*. I. A voltage- and time-dependent component. *J. Membrane Biol.* **89:**139–152

Tyerman, S.D., Findlay, G.P., Paterson, G.J. 1986b. Inward membrane current in *Chara inflata*. II. Effects of pH, Cl^- channel blockers and NH_4^+ and significance for the hyperpolarized state. *J. Membrane Biol.* **89:**153–161

Wang, J., Spieß, I., Ryser, C., Zimmermann, U. 1997a. Separate determination of the electrical properties of the tonoplast and the plasmalemma of the giant-celled alga *Valonia utricularis:* Vacuolar perfusion of turgescent cells with nystatin and other agents. *J. Membrane Biol.* **157:**311–321

Wang, J., Sukhorukov, V.L., Djuzenova, C.S., Zimmermann, U., Müller, T., Fuhr, G. 1997b. Electrorotational spectra of pro-

toplasts generated from the giant marine alga *Valonia utricularis*. *Protoplasma* **196:**123–134

Zimmermann, U. 1978. Physics of turgor- and osmoregulation. *Annu. Rev. Plant Physiol.* **29:**121–148

Zimmermann, U., Büchner, K.-H., Benz, R. 1982. Transport properties of mobile charges in algal membranes: Influence of pH and turgor pressure. *J. Membrane Biol.* **67:**183–197

Zimmermann, U., Steudle, E. 1974. The pressure-dependence of the hydraulic conductivity, the membrane resistance and membrane potential during turgor pressure regulation. *J. Membrane Biol.* **16:**331–352

Zimmermann, U., Steudle, E., Lelkes, P.I. 1976. Turgor pressure regulation in *Valonia utricularis*. *Plant Physiol.* **58:**608–613